

**Polariton pulse propagation at exciton resonance in CuCl: Polariton beat and optical precursor**

M. Sakai, R. Nakahara, J. Kawase, H. Kunugita, and K. Ema  
*Department of Physics, Sophia University, Tokyo 102-8554, Japan*

M. Nagai\* and M. Kuwata-Gonokami  
*Department of Applied Physics, The University of Tokyo, Tokyo 113-8656, Japan*  
 (Received 16 April 2002; published 16 July 2002)

We observed polariton beats and optical precursors in propagation experiments at exciton resonance in CuCl, and obtained good agreement between experimental results and numerical calculations using a two-oscillator model. The observation of more than thirty periods of beatings enables us to determine the polariton parameters and the dephasing constants. At higher intensities we observed a suppression of the polariton beat and found that the suppression is well reproduced by excitation induced dephasing.

DOI: 10.1103/PhysRevB.66.033302

PACS number(s): 78.47.+p, 42.50.Md, 71.36.+c, 42.25.Bs

The problem of light pulse propagation in the resonant region has been extensively studied in atomic gases and semiconductors. Interesting and unusual phenomena such as self-induced transparency (SIT),<sup>1</sup> electromagnetically induced transparency (EIT),<sup>2</sup> and lossless superluminal propagation<sup>3</sup> have been observed in atomic gases. For such novel propagation phenomena, coherent nonlinear interactions between light and matter are essential. Similar coherent propagation phenomena have been rediscovered at the exciton resonance in semiconductors, for example, Rabi flopping,<sup>4</sup> self-induced transmission,<sup>5</sup> and solitonlike propagation.<sup>6,7</sup> While coherent light-propagation physics in atomic gases can be modeled by noninteracting two-level<sup>1,8</sup> or three-level systems,<sup>2</sup> pulse propagation at an exciton resonance in semiconductors is a more complicated problem due to the many-body effects of the electron-hole excitations. Therefore an investigation of pulse propagation at the exciton resonance is of great importance for the understanding of light-matter interactions in many-body systems.

In the linear propagation region, the exciton-light systems form exciton-polaritons that are split into two branches (upper and lower branches). If the spectrum of an input pulse is broad enough to cover both branches, the interference between the upper and the lower polariton modes produces a beat in the temporal shape of the propagated pulse, the so-called polariton beat. A clear observation of the polariton beat means that both modes of polariton propagate coherently across the whole length of the sample. Therefore we can derive several characteristics of the excitons from the polariton beat. For example, we can estimate the oscillator strength of the exciton from the periods of the beat<sup>9</sup> with almost the same accuracy as high-resolution frequency-domain experiments. We can also obtain information on the damping rate of the polariton which is difficult to obtain by the frequency-domain experiments, because the coherence between both polariton modes is strongly affected by the damping rate, i.e., the dephasing process of the exciton-polariton system.

At increased pulse intensities, it is known that the polariton beating is suppressed by the increased dephasing process due to incoherent exciton-exciton interactions.<sup>10-12</sup> Thus the suppression of the polariton beats in the nonlinear region

includes important information on the many-body effects. In the past experimental demonstrations on polariton beats, however, the periods of the beatings were very long due to the small longitudinal-transverse (LT) splitting energies of the excitons, and thus the number of observable beatings was too small to allow analyzing the beating properties in detail.

In the present study, we performed pulse propagation experiments just at the  $Z_3$ -exciton resonance of CuCl and observed very clear polariton beats. Since the exciton in CuCl has a very large LT splitting energy, more than one order of magnitude larger than the dephasing energy, a great number of beatings can be observed. By fitting the observed beatings to a calculation over a range of more than thirty beating periods, we determined the parameters of polariton dispersion and obtained good agreement with the values determined by frequency-domain experiments. With increasing input-pulse intensity, strong suppression of the polariton beats was observed as previously reported for other materials. We attribute this suppression to excitation-induced dephasing (EID),<sup>13</sup> and again obtained good agreement with calculations using the propagation equation.

In addition to the polariton beat, we could observe a precursor in front of the main polariton pulse, since the input spectrum extended into the region where polariton dispersion is almost linear. For such a case it was theoretically predicted that a fast front of the pulse travels with a speed of  $c/\sqrt{\epsilon_\infty}$  (the Sommerfeld precursor<sup>14</sup> due to the high-frequency part of the initial pulse) or of  $c/\sqrt{\epsilon_0}$  (the Brillouin precursor<sup>15</sup> due to the low-frequency components of the initial pulse). Here  $c$  denotes the velocity of light in vacuum, and  $\epsilon_\infty$  and  $\epsilon_0$  are the dielectric constants at the higher and lower frequency limits. Precursors of microwaves<sup>16</sup> and magnetostatic waves<sup>17</sup> have been observed experimentally, however, precursors in the optical region are difficult to observe because of the high carrier frequency. Although there have been a few reports on the experimental observation of optical precursors,<sup>4,18</sup> a clear peak separation from the main pulse has not been observed and an analysis of precursors has not been attempted. In the present study, we observed the precursor component clearly and found that the observed precursor consists of the lowest-frequency part of the input pulse. The precursor is hardly influenced by many-body ef-

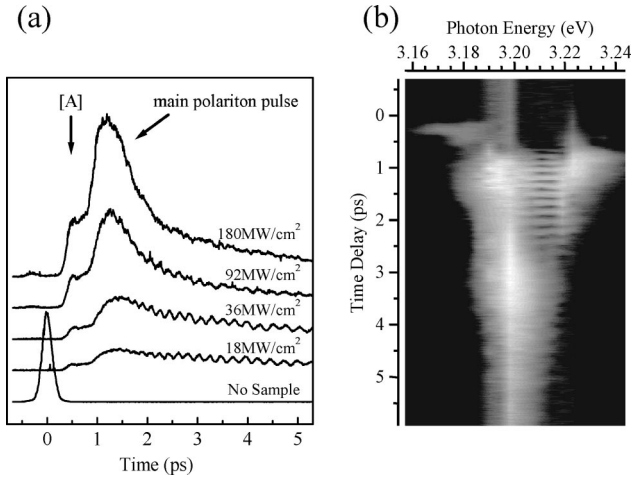


FIG. 1. (a) Measured transmitted pulse shapes for different input-pulse intensities. The time scale has been set to the arrival of the pulse without sample. A characteristic peak [A] and a main broad polariton pulse with explicit polariton beats are observed. (b) Frequency resolved measurement at an intermediate intensity ( $\sim 40$  MW/cm<sup>2</sup>). We can easily see that the precursor component consists of the lowest-frequency part.

fects because of the large detuning from the resonance; thus it can be used as a marker in the temporal shape at high input intensities where the polariton pulses are greatly modified by the many-body nonlinear effects.

The experiments were performed at 10 K using a high purity single crystal of CuCl with a thickness of 3.4  $\mu\text{m}$ . For the input pulse, we used second harmonic generation (SHG) of a regenerative Ti:sapphire amplifier whose center frequency was set just at the center energy of the LT splitting of the  $Z_3$  exciton (3.204 eV). Since the transmitted pulse shape is influenced by a frequency chirp of the input pulse, the chirp was carefully compensated by a combination of a grating pair and a prism pair. Thus the pulse was almost transform limited. Its temporal width is 150 fs and energy width is 11 meV which covers the LT splitting energy of the  $Z_3$  exciton. The temporal shapes of the transmitted pulses were measured by a down-conversion technique using a fundamental pulse of the regenerative Ti:sapphire amplifier as a reference pulse, and the frequency resolved measurements were done using an optical Kerr-shutter technique.

Figure 1(a) shows the transmitted pulse shapes for different input-pulse intensities. We found two characteristic components, an optical precursor labeled [A] and the main polariton pulse. We observed explicit polariton beats in the main broad polariton pulse at low input intensity. The number of the beatings is larger than in any other materials reported so far. Increasing the intensity, we observed suppression of these polariton beats clearly. Figure 1(b) shows the frequency resolved measurements of the transmitted pulses at intermediate intensity. The polariton beat appears in the region of the LT gap and that the precursor consists of the lowest-frequency part of the transmitted pulse. Therefore the observed precursor is a kind of Brillouin precursor. However, it is hard to observe the Sommerfeld precursor in the  $Z_3$ -exciton resonant region because another resonance of the

TABLE I. (a) Fixed and (b) fitted parameters used in numerical calculations. Here  $m_0$  is the rest mass of the electron.

(a)			
$\Omega_{3T}$	$\Omega_{12T}$	$\varepsilon_b$	$M_3$
3.2022 eV	3.270 eV	4.3	$2.3 m_0$
(b)			
$4\pi\beta_3$	$4\pi\beta_{12}$	$\gamma_3$	$\gamma_{12}$
$4.618 \times 10^{-3}$	$1.165 \times 10^{-2}$	0.12 meV	10.0 meV

$Z_{1,2}$  exciton exists just above the  $Z_3$  exciton. The clear appearance of the Brillouin precursor is due to the fact that the input pulse spectrum has a long low-energy tail with some structure. The condition for a clear appearance of precursors is determined by a complicated relation between the spectrum-tail shape and the polariton dispersion in the tail region.<sup>19</sup> Actually the heights and positions of the precursors were sensitive to the alignment of the laser and the SHG system both of which affect the input spectrum shape.

In order to analyze the observed polariton beats at low intensity, we used a two-oscillator model<sup>20</sup> in which the  $Z_{1,2}$ -exciton state is included in addition to the  $Z_3$ -exciton state. In our study, the spatial dispersion is included only in transverse energy of the  $Z_3$  exciton. Therefore the dielectric function of our model is given as

$$\varepsilon(\omega) = \varepsilon_b + \frac{4\pi\beta_{12}\Omega_{12}^2}{\Omega_{12}^2 - \omega^2 - i\omega\gamma_{12}} + \frac{4\pi\beta_3\omega_3^2}{\omega_3^2 - \omega^2 - i\omega\gamma_3}, \quad (1)$$

$$\omega_3 = \Omega_3 + \frac{\hbar k^2}{2M_3}, \quad (2)$$

where  $\varepsilon_b$  is the high-frequency dielectric constant,  $\Omega_i$  and  $\gamma_i$  ( $i=3$  or  $12$ ) are the transverse energies and the dephasing constants of the  $Z_i$  exciton, respectively, and  $M_3$  is the effective mass of the  $Z_3$  exciton. Parameters  $4\pi\beta_i$  characterize the oscillator strength, and are related to the LT splitting energies. Since periods and phases of the beats are very sensitive to the oscillator strength of the  $Z_3$  exciton, we can determine  $4\pi\beta_3$  to a very high accuracy by fitting to the experimental results. The fixed parameters<sup>21</sup> of the calculation and the fitted parameters are listed in Table I. The parameters obtained are in agreement with the values determined by frequency-domain experiments. Note that the values of the energies of the longitudinal excitons were not used in the calculation, but they appear when  $\varepsilon(\omega)$  is set to zero for  $\gamma_i \rightarrow 0$ . The derived value of the LT splitting energy of the  $Z_3$  exciton is also in agreement with the obtained value previously<sup>21</sup>  $\Delta_{LT} = 5.7$  meV.

To demonstrate the beat periods and phases we compare the differentiated data in Fig. 2(a). It shows the good agreement between the experiment and the calculation based on the two-oscillator model. Figure 2(b) demonstrates discrepancies in phase and amplitude between experiment and calculation separately for each beat. The phase shifts  $\Delta_{\text{phase}}$

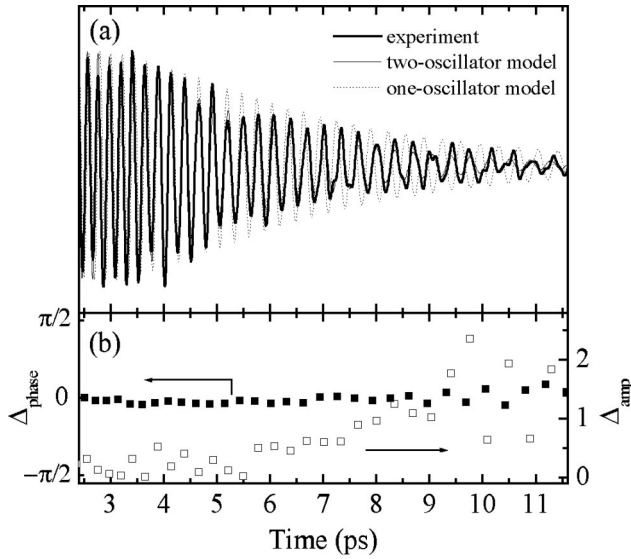


FIG. 2. (a) Differentiated beatings of the experimental result (thick line), together with fits based on a two-oscillator model (thin line, almost indistinguishable from the experiment), and on a one-oscillator model (dotted line). (b) Difference between experimental result and calculation based on the two-oscillator model. Filled squares show the phase shift  $\Delta_{\text{phase}}$  and open squares show the deviation of the modulation amplitude  $\Delta_{\text{amp}}$  separately for each beat of the experimental and calculational results.

(filled squares) are in the range of  $-\pi/12$  to  $\pi/12$  for more than thirty beating periods which gives a precision of the oscillator strength of  $\pm 0.3\%$ . This high precision arises from fitting to the whole features of the polariton beats which, in turn, come from coherent interferences over a wide range of both branches. On the other hand, the deviation of the modulation amplitude  $\Delta_{\text{amp}}$  (open squares)—which shows the precision of the dephasing  $\gamma_i$ —exceeds 1 in the pulse tail region. This discrepancy is mainly due to the small signal-to-noise ratio in the tail region, but there is another intrinsic reason: the beatings in the tail region come from slow group velocity components of both polariton modes. The damping rates of such slow polaritons in or near the LT gap are expected to deviate from those derived by the dielectric function.

The dotted line in Fig. 2(a) shows the calculated beating using a one-oscillator model with  $\Delta_{\text{LT}} = 5.7$  meV. It clearly shows a large discrepancy with the experimental data. With the one-oscillator model, no set of parameters could be found that would allow a good fitting over the whole range. It indicates that the polariton dispersion in CuCl can only be described by a two-oscillator model as has been pointed out by frequency-domain experiments.<sup>22</sup>

In our calculation, we use Pekar's additional boundary condition (ABC) (Ref. 23) to determine the amplitude ratio of the upper and lower polariton branches. There have been a great number of debates on the ABC problem.<sup>24</sup> In our calculation, however, the important features of the polariton beating (periods and phases of the beatings) are not affected by the selection of the ABC, although the modulation depth of the beating changes slightly with ABC.

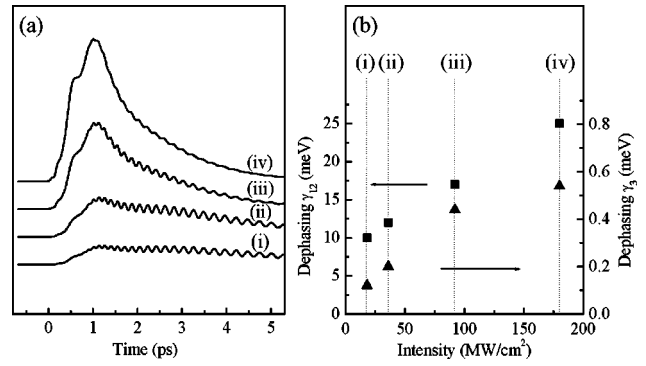


FIG. 3. (a) Numerical fittings using different pairs of dephasing constants  $\gamma_3$  and  $\gamma_{12}$ . (b) Values of dephasing constants used for the fittings. The intensity axis corresponds to the intensities of the experimental results Fig. 1(a).

As shown in Fig. 3(a), the calculations reproduce not only the beat properties but also the whole transmitted pulse shape when appropriate dephasing constants are used. They also reproduce the optical precursor qualitatively because the experimental spectrum which includes the long low-energy tail was used in the calculations. The suppression of the polariton beat at higher intensities can also be reproduced when the dephasing constants are increased. In previous studies the suppressions were explained by the density-dependent asymmetry dephasing<sup>12</sup> or an interaction of the single exciton states with the two-exciton continuum.<sup>11</sup> Such incoherent exciton-exciton interactions yield additional dephasing of the excitonic polarization. Therefore we analyzed the suppression of the polariton beats with a simple model in which all many-body effects on the polariton beat were pushed into the EID. In the formalism of semiconductor Bloch equation (SBE), EID is modeled by including a density-dependent term in the imaginary part of the dynamically screened Hartree-Fock self-energies. Specifically, at low excitation intensities, the dependence of the dephasing rate on the exciton density  $n_{\text{ex}}$  can be expressed as<sup>13</sup>

$$\gamma = \gamma^0 + \gamma' n_{\text{ex}}, \quad (3)$$

where  $\gamma^0$  is the homogeneous linewidth at zero exciton density and  $\gamma'$  is the scattering cross section. The second term of the right side represents EID. Figure 3(b) shows the dephasing constants which best reproduced the experiments at each intensity. The obtained dephasing constants obey Eq. (3) at low intensities. Although a difference between experiments and calculations in the intensity of the precursor at higher intensities may arise from our simple analysis, at least the EID explains the suppression of the beats qualitatively. Further analysis using a modified SBE is expected to result in an improved quantitative agreement.

Note that the largest intensity of the traces in Fig. 1(a) is well below the exciton Mott transition intensity<sup>25</sup> of several  $\text{GW}/\text{cm}^2$ . Finally we performed a few confirming measurements and calculations on the intensities in our experiments. In order to find the range of the  $\chi^{(3)}$  nonlinearity, we performed two-pulse four-wave-mixing (FWM) measurements. The FWM signal intensity increases in proportion to the third

power of the input intensity up to  $\sim 40$  MW/cm<sup>2</sup> and saturates at higher intensities. Thus beat suppression starts around the boundary region of the  $\chi^{(3)}$  nonlinearity. We also calculated the transmitted pulse shapes using a nonlinear propagation equation in the frequency domain with the  $\chi^{(3)}$  nonlinearity. The results show that the increase of intensity leads to a shift in the temporal phase of the beatings but not to a suppression. Thus we reconfirmed that pulse propagation in the nonlinear region is mainly dominated by the incoherent EID effect, not by the coherent  $\chi^{(3)}$  nonlinearity.

In conclusion, we observed polariton beats and optical

precursors by propagation experiments at exciton resonance in CuCl and obtained good agreement between experimental results and numerical calculations using a two-oscillator model. Suppression of polariton beats was observed in the nonlinear region. Fittings to the experimental results are given, that obtain good agreement between the experimental results and EID-based calculations.

The authors would like to thank Dr. L. Boesten for the careful reading of the manuscript. This work was partly supported by a Grant-in-Aid from the Ministry of Education, Culture, Sports, Science and Technology of Japan.

\*Present address: Department of Physics, Graduate School of Science, Kyoto University, Kyoto 606-8502, Japan

<sup>1</sup>S. L. McCall and E. L. Hahn, Phys. Rev. **183**, 457 (1969).

<sup>2</sup>S. E. Harris, J. E. Field, and A. Imamoglu, Phys. Rev. Lett. **64**, 1107 (1990).

<sup>3</sup>L. J. Wang, A. Kuzmich, and A. Dogariu, Nature (London) **406**, 277 (2000).

<sup>4</sup>N. C. Nielsen, S. Linden, J. Kuhl, J. Förstner, A. Knorr, S. W. Koch, and H. Giessen, Phys. Rev. B **64**, 245202 (2001).

<sup>5</sup>H. Giessen, A. Knorr, S. Haas, S. W. Koch, S. Linden, J. Kuhl, M. Hetterich, M. Grun, and C. Klingshirn, Phys. Rev. Lett. **81**, 4260 (1998).

<sup>6</sup>K. Ema and M. Kuwata-Gonokami, Phys. Rev. Lett. **75**, 224 (1995).

<sup>7</sup>M. Sakai, K. Sano, H. Kunugita, and K. Ema, J. Nonlinear Opt. Phys. Mater. **9**, 63 (2000).

<sup>8</sup>L. Allen and J. H. Everly, *Optical Resonance and Two-Level Atoms* (Dover Publications, New York, 1987).

<sup>9</sup>D. Fröhlich, A. Kulik, B. Uebbing, A. Mysyrowicz, V. Langer, H. Stolz, and W. von der Osten, Phys. Rev. Lett. **67**, 2343 (1991).

<sup>10</sup>D. Fröhlich, A. Kulik, B. Uebbing, V. Langer, H. Stolz, and W. von der Osten, Phys. Status Solidi B **173**, 31 (1992).

<sup>11</sup>J. Förstner, A. Knorr, S. Kuckenburg, T. Meier, S. W. Koch, H. Giessen, S. Linden, and J. Kuhl, Phys. Status Solidi B **221**, 453 (2000).

<sup>12</sup>J. S. Nägerl, B. Stabenau, G. Bohne, S. Dreher, R. G. Ulbrich, G. Manzke, and K. Henneberger, Phys. Rev. B **63**, 235202 (2001).

<sup>13</sup>Y. Z. Hu, R. Binder, S. W. Koch, S. T. Cundiff, H. Wang, and D. G. Steel, Phys. Rev. B **49**, 14 382 (1994).

<sup>14</sup>A. Sommerfeld, Ann. Phys. (N.Y.) **44**, 177 (1914).

<sup>15</sup>L. Brillouin, Ann. Phys. (N.Y.) **44**, 204 (1914).

<sup>16</sup>R. A. Alvarez, D. P. Byrne, and R. M. Johnson, Rev. Sci. Instrum. **57**, 2475 (1986).

<sup>17</sup>D. D. Stancil, J. Appl. Phys. **53**, 2658 (1982).

<sup>18</sup>J. Aaviksoo, J. Kuhl, and K. Ploog, Phys. Rev. A **44**, R5353 (1991).

<sup>19</sup>M. Sakai, R. Nakahara, J. Kawase, H. Kunugita, and K. Ema (unpublished).

<sup>20</sup>E. Tokunaga, K. Kurihara, M. Baba, Y. Masumoto, and M. Matsuoka, Phys. Rev. B **64**, 045209 (2001).

<sup>21</sup>T. Mita, K. Sôtome, and M. Ueta, Solid State Commun. **33**, 1135 (1980).

<sup>22</sup>E. Ostertag, Phys. Rev. Lett. **45**, 372 (1980).

<sup>23</sup>S. I. Pekar, Sov. Phys. JETP **6**, 785 (1958).

<sup>24</sup>H. C. Schneider, F. Jahnke, S. W. Koch, J. Tignon, T. Hasche, and D. S. Chemla, Phys. Rev. B **63**, 045202 (2001), and references therein.

<sup>25</sup>M. Nagai, R. Shimano, and M. Kuwata-Gonokami, J. Lumin. **87-89**, 192 (2000).